

**BEAM COMBINATION IN A MULTI-TELESCOPE, MONOLITHIC INTERFEROMETER****E N Ribak, E B Hochberg, N A Page, S P Synnott, J B Breckinridge**

Jet Propulsion Laboratory  
California Institute of Technology  
4800 Oak Grove Drive  
Pasadena, CA 91109

**ABSTRACT**

Two approaches are considered when combining the beams of many small telescopes mounted on a single structure: direct imaging and pupil plane interferometry. We used first-order optical design and computer simulation to compare the two methods. Direct imaging allows larger telescopes, whereas pupil plane combination provides high spectral dispersion. Both require large detectors and large telescope magnifications, have many reflections per path, and provide a limited field-of-view. A pair-wise combination scheme is proposed, which improves the signal-to-noise ratio and reduces the detector size for pupil-plane combination.

**1. Introduction.**

We examine the case of an interferometer comprised of a number of small telescopes mounted in the same structure. Currently there are three approaches to beam combination from these telescopes: (I) The imaging scheme, where the beams are arranged in a scaled version of the telescopes and form an image on the detector (MMT, COSMIC) [Beckers *et al.* 1983, Traub *et al.* 1982]. This scheme requires a fully phased interferometer. (II) the pupil plane scheme, which

interferes the beams at their exit pupil, and spatial or temporal modulation of the fringes allows their detection. This method applies in the case of a coherent interferometer. (III) The fibre scheme, which utilises fibres to lead the light from the foci of the telescopes to the vicinity of the detector, at which point one of the first two schemes can be employed (FLOAT, OASIS) [Connes *et al.* 1987, Noordam *et al.* 1987]. It turns out that most of the factors that constrain our interferometer also lead to similar parameters in either one of the three above-mentioned systems. We were able to quantify some of these relations for our case of a space interferometer.

## 2. Assumptions.

It is clear that a multi-telescope interferometer should yield high resolution images. What should drive us to put one in space? The main advantage is due to the fact that we do not have any atmosphere to disrupt the wave-front or absorb some of the light. Thus we should strive to have long integration times and to observe at wave-lengths not possible from the ground. Unfortunately we have some severe offsets even with these two obvious factors. It so turns out that a free-floating space interferometer might have undamped vibrations of frequencies and magnitudes that current theory and software cannot predict (although the vibration problem can be alleviated by putting it on the moon). As regards wave-length, there is not much point in going to the infra-red. This is because atmospheric coherence size and time are not the limiting factors in this regime. Also, there are numerous clear windows, which do allow observing in the infra-red through the atmosphere.

Both atmospheric turbulence and opacity are strong limiting factors in the visible and ultra-violet. Therefore, this seems to be the region of frequency we should try and employ in space. However, higher accuracy in our wave-front monitoring and control is required, since the wave-length is shorter. The number of reflections in each beam becomes important, since the reflection of visible-ultra-violet mirrors is low. Alternatively, it requires the development high-transmission fibres for the ultra-violet. Finally, it should be pointed out that current astrophysical knowledge and theory render most ultra-violet objects unresolvable on the milliarcsecond scale we are talking about.

We chose a range of 100 to 1000 nm as our goal. We also assumed that the interferometer maximum base-line can span at most some 30 m, after opening up during space deployment. It is supposed to deploy autonomously, with pre-aligned optics.

## 3. Optical design.

Starting with the detector, and propagating backwards to the collecting telescopes, we calculated a unified set of first-order optical design parameters for the imaging interferometer and the pupil plane interferometer. The limiting optical factors were the number of reflections per beam and the magnification of the telescopes. In the latter case we found that the magnifications could be minimised by catenating or "clumping" a number of telescopes into one phased unit. This requires that all telescopes in the unit should have the same phase, and thus behave as a single, larger telescope. This is to be compared with the non-redundant scheme, where all the telescopes are not fully phased, and the phase information comes through internal (metrology) or external (stellar) referencing. In the imaging case all the telescopes are fully and actively phased by referencing. Some of the parameters of the optical design can be found in the following table.

	pupil plane non-redundant	pupil plane partial redundant	image plane
maximum base-line	30 m	30 m	30 m
central mast	15 m	15 m	15 m
wave-length range	0.1 – 1.0 $\mu\text{m}$	0.1 – 1.0 $\mu\text{m}$	0.1 – 1.0 $\mu\text{m}$
pixel size	10 $\times$ 10 $\mu\text{m}^2$	10 $\times$ 10 $\mu\text{m}^2$	10 $\times$ 10 $\mu\text{m}^2$
detector size	100 $\times$ 3 $\text{mm}^2$	100 $\times$ 3 $\text{mm}^2$	43 $\times$ 43 $\text{mm}^2$
pixels/fringe <sup>(1)</sup>	4	4	2
number of telescopes	24	24	24 <sup>(2)</sup>
primary aperture	50 cm	50 cm	100 cm
full field-of-view	1.5 arcsec	1.5 arcsec	1.5 arcsec
reflections/path <sup>(3)</sup>	7	7	8
telescope groups	24	4	24
telescopes/group	1	6	1
non-redundant frequencies	276	6 <sup>(4)</sup>	276
telescope magnification	90	16.25	30
secondary aperture	7.6 mm	30.77 mm	33.33 mm
combiner magnification	18	3.25	– NA –

Notes:

- (1) The number of pixels per fringe for the highest frequency, which is the one that matters, may be dropped to less than four. This is if we associate it with a pair of telescopes of the shortest distance and the highest contrast. Thus the furthest beams come from the closest telescopes. As the object is slightly resolved on this base-line, the fringe contrast is high and allows to have down to two pixels per fringe. Less pixels will enable us to relax some of the other parameters. For the imaging case we assumed two pixels per resolution element.
- (2) The number of telescopes in the imaging case can be increased without changing the other parameters.
- (3) The large number of reflections per beam (7 to 8) will require wide-band mirrors, with high reflection extending to 100 nm.
- (4) The calculation for the partially redundant pupil plane was done with all 24 telescopes along one line.

#### 4. Non-redundant beam combination.

While combining a large number of beams in a spatial (or temporal) non-redundant output array we encounter a number of severe problems, the most notable being the very high ratio of the maximum frequency to the minimum frequency. This high ratio requires an exceptionally large detector, holding many small pixels. A related problem is the large throw distance required to separate the beams when looking back from the detector. The telescope magnifications obtained from the analysis lead to very tight fabrication and assembly tolerances.

Using non-redundant temporal combination solves the optical problems, since now the telescopes are allowed to be adjacent, and the spectral dispersion is smaller. But it rules out the possibility of large dynamic range integrating detectors, such as a CCD. And the problems of

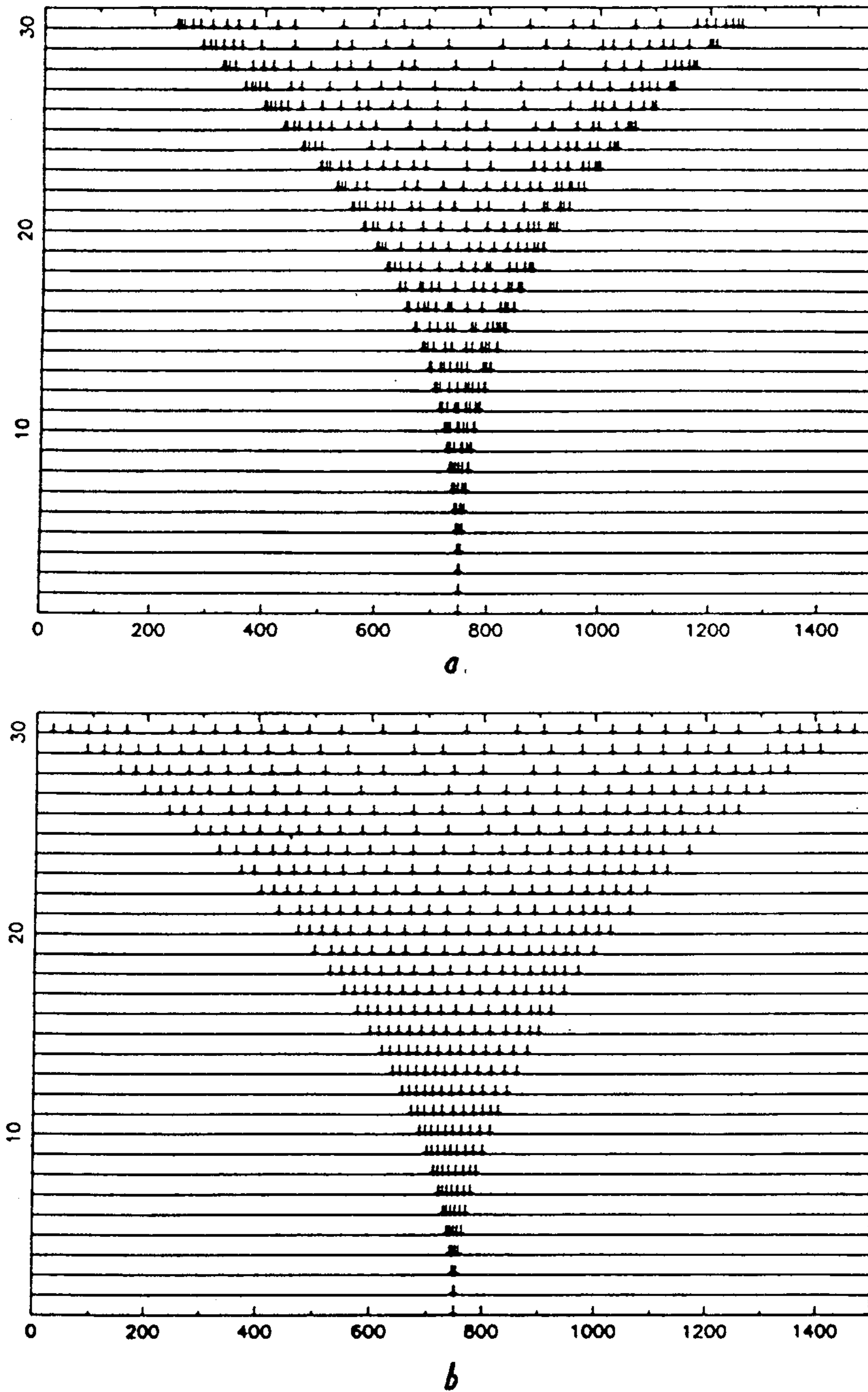


Figure 1. Location of 2 - 30 beams in the exit pupil of a non-redundant beam combiner. (a) The shortest spacing is one unit. (b) The shortest spacing is  $N$  units, where  $N$  is the number of beams. The ratio of longest to shortest spacing is improved (by a factor  $\approx N$ ).

highest-to-lowest frequency ratio is the same, only it is now temporal instead of spatial frequency.

Essentially, the problem can be summarised as follows: For  $N$  telescopes, the number of base-lines is  $B = N(N - 1)/2$ . Thus, if the shortest base-line is one unit, then the incoming beams are spread over  $S$  units, where  $S > B$  for  $N > 4$ . For even higher values the span behaves more like  $N^{2.5}$ . As a result, the ratio of the longest to shortest base-line is  $R = S/1$ . For 30 beams,  $S \approx 1000$ , an intolerably high value. Fig. 1a shows such values, optimised by means of a Monte-Carlo program.

The solution lies in the recognition that the shortest base-line does not have to be one unit; it can be longer. In other words, the longer base-lines are not an integer sum of the shortest one. If we restrict the shortest base-line to be of length  $L$ , the shortest span can be  $S = (N - 1)(N/2 + L - 1)$ . The ratio of the longest to shortest base-lines turns out to be  $R = S/L = (N^2 - 3N + 2)/2L + N - 1$ . For example, for  $L = N/2$  we get  $R = 2N - 4 + 2/N$ , a plausible value. Now suppose the shortest base-line,  $L$ , creates  $F$  fringes across the detector. We have

base-line	length	fringes	fringes $L \approx 1, F = S/L$	fringes $L \gg 1, F = 1$
longest	$S$	$FS/L$	$S$	$S/L$
next longest	$S - L$	$F(S - L)/L$	$S - L$	$(S - L)/L$
shortest	$L$	$F$	$L$	1

Leakage is a severe problem when we try to differentiate between different base-lines. The source of leakage is a non-integer number of fringes across the detector. When estimating the fringe amplitude and phase, one usually utilises Fourier plane analysis: the fringe pattern is transformed, and every fringe pattern turns into a complex number, signifying its amplitude and phase. The location of this signal is within one Fourier component for discrete transforms and an integer number of cycles [Walkup and Goodman 1973, Greenaway 1985]. If the number of cycles is not an integer, the analytical repetition of the fringe pattern (as assumed in Fourier transforms) will lead to phase jumps at the pattern end. This results in ambiguity of the exact frequency of the signal, or leakage into neighbouring Fourier components. The width of the signal will be inversely proportional to the number of detector pixels and directly proportional to the amount of mismatch in phase at the detector edge.

The way to contend with leakage is clear: have as many pixels as possible, and as little mismatch at the detector end as possible. The mismatch can be solved by analytic continuation of the (known) pattern across the end up to a whole fringe. This is done by duplicating a few pixels with the right phase from inside the pattern at the edge until a full number of cycles is achieved (fig. 2). If the number of cycles is large, one can ignore the last few pixels, so as to have again an integer number of cycles.

As mentioned, the ratio of longest to shortest base-lines,  $R$ , is small. The width of each frequency band is the reciprocal of the number of pixels across the detector (namely  $1/4R$ ), and should be kept as narrow as possible. These two requirements are in contradiction, and as a compromise we chose for the shortest base-line  $L = N$  units, where  $N$  is the number of telescopes. In this case the span is  $S = (N - 1)(3N/2 - 1)$ , and  $R \approx 3N/2$  for large  $N$ . This also fulfils the requirement that the band width is narrow (it is  $\approx 2/3N$ ). Fig. 1b shows a Monte-Carlo optimised beam organisation.

The sensitivity of the pupil-plane non-redundant scheme was tested by a computer simulation. The extended object chosen (fig. 3) was made out of a combination of Gaussians and point sources, and characterised by 24 parameters. This high complexity led to an average visibility of  $10^{-3}$  over the  $uv$  plane. Twenty-five telescopes were arranged on a Mill's cross, and a few non-redundant snap-shot measurements were taken at different light levels. The output beam array was figured in

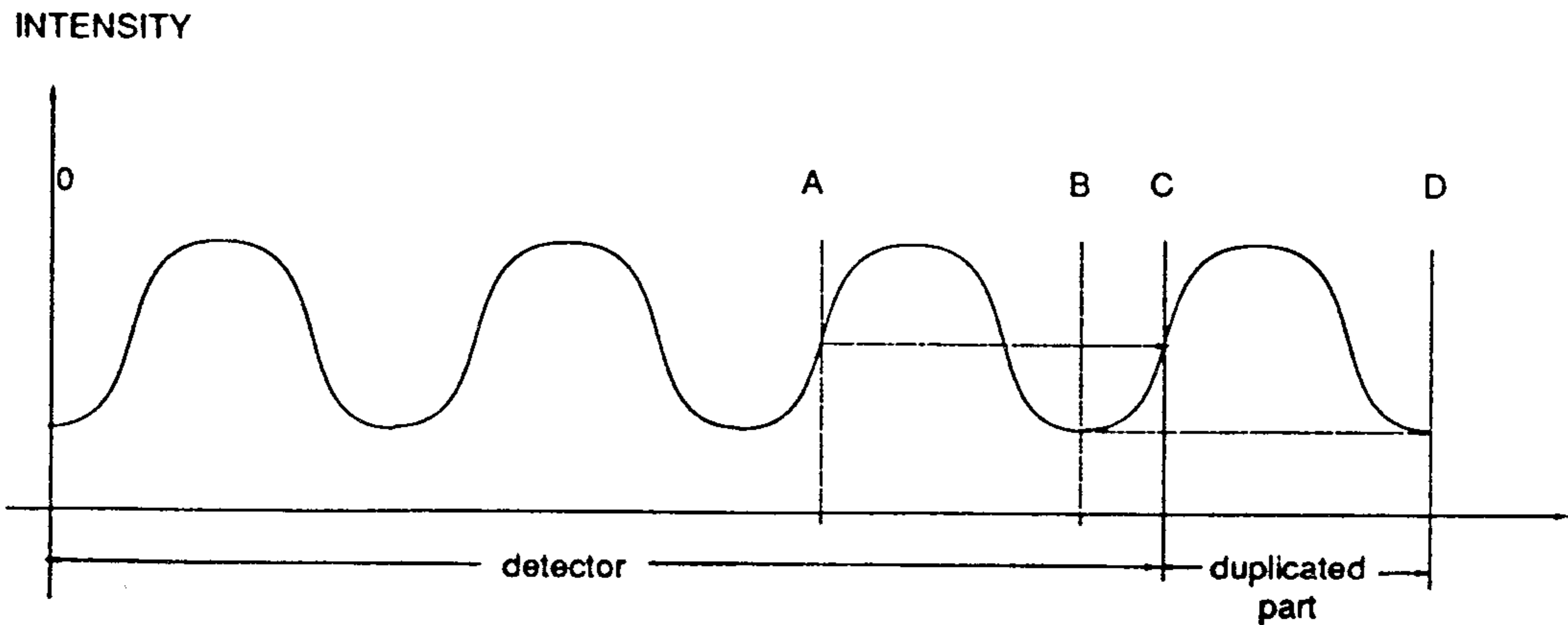


**Figure 2.** Fringes across a detector. If the number of cycles is not an integer, duplication of a part of the fringe can reduce leakage. This is achieved by appending the measured section  $AB$  to the detector end, at  $CD$ . Alternatively, if the number of cycles is large enough, the last pixels ( $BC$ ) can be ignored before performing the analysis.

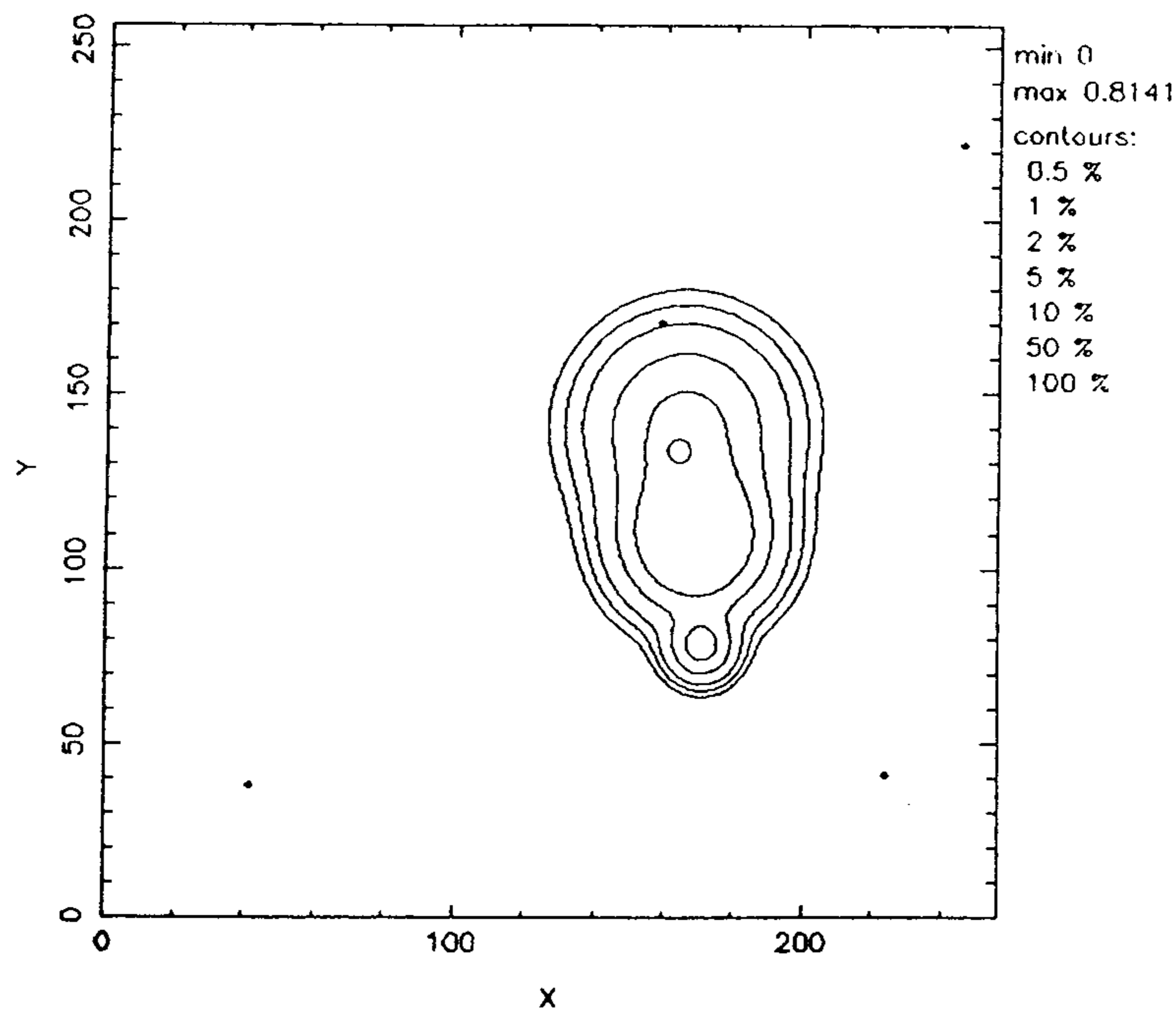


**Figure 3.** An extended object for simulation of the performance of the non-redundant beam combination scheme. The object is composed of 4 point sources and 3 Gaussians.

a non-redundant order, with  $L = N$ , and served to illuminate a linear detector, where the fringes were registered. Poisson noise was then added to each pixel, according to the total light level at that point.

Once the detector was read out, the data were analysed: the fringe amplitudes and phases were extracted by Fourier transform techniques. Since the input data were known, a comparison

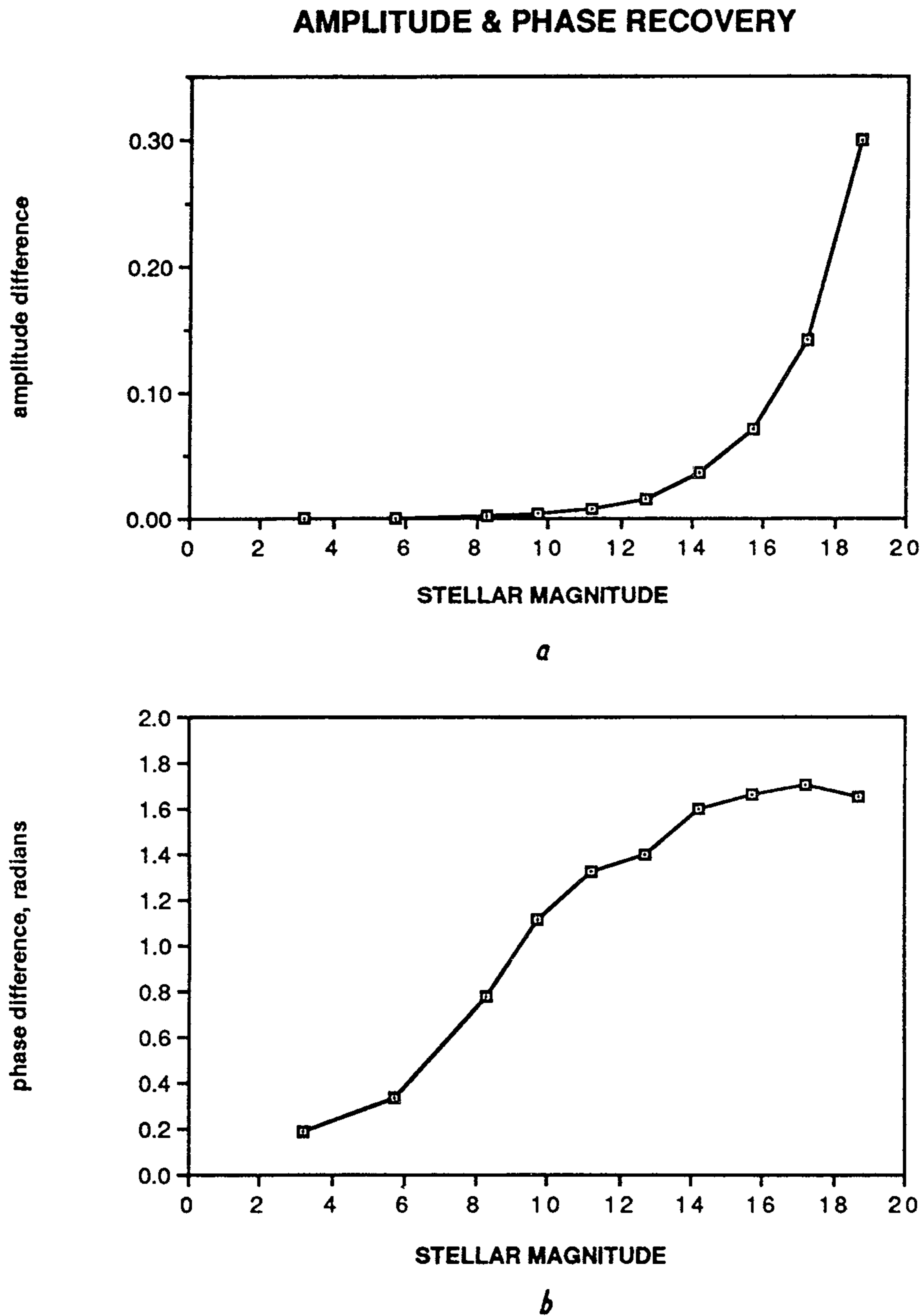


**Figure 4.** Amplitude and phase recovery from a 25-beam non-redundant array. (a) Magnitude of the average difference vector (input visibility – output visibility). (b) Average phase difference (input phase – output phase). The corresponding number of photons was  $10^8$  for magnitude 12, under the assumptions that  $\Delta\lambda = 20$  nm, the efficiency was 20%, the integration time was 100 sec, the number of telescopes was 25, and their diameter 0.5 m.

between input and output data was straightforward. We averaged the results over the 300 baselines measured, in order to be able to estimate the robustness of the technique to the light level. The error on the visibility amplitude was less than 10% down to a total level of  $10^5$  photons, below which it rose slowly (fig. 4a). The error on the phases was much higher (fig. 4b): it reached 1 radian at  $5 \times 10^7$  photons, and continued climbing for lower intensities. This level corresponds to stellar magnitude 12, under the assumptions that  $\Delta\lambda = 20$  nm, the overall system efficiency is 20%, and that the integration time is 100 sec, achieved by using a reference star or internal metrology. It should be pointed out that 25 telescopes of 0.5 m diameter have the same aperture area as the Hubble space telescope.

### 5. Pair-wise beam combination.

As we saw above, non-redundant beam combination has its problems: it requires large-format detectors and awkward optics, and returns low signal-to-noise results. In order to overcome these, we propose here a solution that is simpler optically, requires a smaller detector and has an improved signal-to-noise (see fig. 5). The idea is as follows: (I) pack all the beams in the exit pupil as close as possible along a line; (II) use an anamorphic element to spread them perpendicular to that line. Thus one has a square made of stripes, each emanating from a different telescope or a fibre optic. (III) Now employ an interferometer to combine two such images of this square, rotated at  $90^\circ$  to each other. The two images interfere on a detector, thus creating a criss-cross pattern of stripes. At each junction point, where two stripes meet, a small number of fringes will be created, whose frequency depends on the interferometer chosen. Each such fringe pattern corresponds to the interference of the two telescopes whose stripes are crossing at this point.

The optical implementation is simple: a cylindrical element spreads the beams in the transverse direction. In the case that the beams are brought from the telescopes by means of mirrors (as opposed to using fibres for leading the light), we might be able to combine the anamorphic element with the other elements along the beam, to save on reflections. The anamorphic element has to spread the beams to an aspect ratio of  $N:1$ , where  $N$  is the number of telescopes. This is the most stringent constraint. The emerging wave-front, however, does not have to be planar, as fringes can be tolerated.

The interferometer employed to separate and recombine the beams can be one of a few choices. It can be a folding shear interferometer, where the folding line is along the diagonal of the pattern, or a  $90^\circ$  rotational shear interferometer with the pattern center coinciding with the interferometer center. For these two cases the wave-fronts are parallel when arriving on the detector, allowing the number of pixels on each side to be equal to the number of telescopes. If the anamorphoser cannot produce plane waves, we will have to allot four pixels for each fringe (and the total number of pixels a few times the number of telescopes). The drawback is that one output of the interferometer is usually lost, and even if collected, it does not necessarily provide more information. Another choice is an interferometer that divides the wave-front, as opposed to the shearing interferometers, which utilise amplitude division. A practical device is Lloyd's mirror, although Fresnel's mirrors or Fresnel's bi-prism can be employed. The drawback of these interferometers is that there is a number of fringes at each cross-point (and, again, more pixels in the detector). The fringe density can be decreased by magnification of the interference pattern.

The signal-to-noise of the pair-wise interferometer is also higher than that of other pupil-plane combinations. We follow here the calculation given by Roddier [1987] for the faint object case. Assume signal-to-noise  $\Lambda$  for a pair of telescopes obtained in time  $T$ . If we couple all the beams ( $N$  in number) in pairs, we get  $N/2$  frequencies, but no phase relations. If we can switch pairs, we can also observe the  $N(N-1)/2$  frequencies in time  $TN$  to get the same signal-to-noise  $\Lambda$ . If we

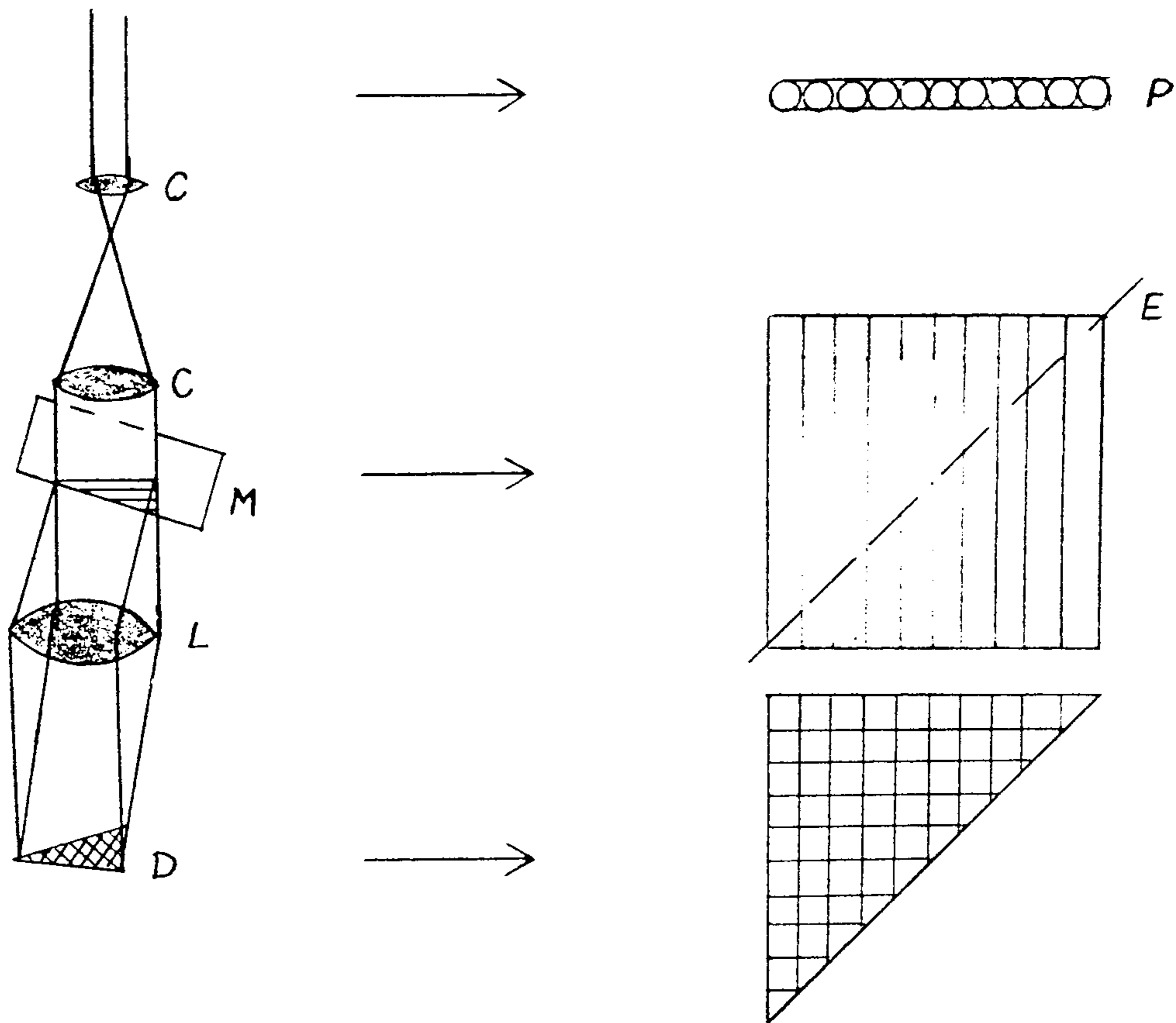


**Figure 5.** Pairwise combination of beams. The beams are lined up in the exit pupil ( $P$ ), stretched orthogonally to form a square, then interfered with  $90^\circ$  rotated same square. The fringes at every junction in the crosswise pattern correspond to a different pair of beams and are parallel to the mirror edge ( $E$ ).  $C$  – cylindrical lenses,  $M$  – Lloyd's mirror,  $L$  – magnifying lens,  $D$  – detector.

combine all with all in a non-redundant fashion, we get  $N(N-1)/2$  frequencies with signal-to-noise  $\Lambda/N$  over the same integration time. Alternatively we can acquire the same signal-to-noise  $\Lambda$  with integration time  $TN^2$ . But if we do the same calculation for the proposed pattern, we reduce the signal at each point by a factor of  $1/N$ , with attendant reduction in signal-to-noise to  $\Lambda/\sqrt{N}$ . This is equivalent to getting signal-to-noise  $\Lambda$  in  $TN$  observation time. So we have the advantage of signal-to-noise as in the pairing case, withing losing the phase information.

Without using fibres, it is very difficult to switch beams. A fibre network similar to that proposed by Connes *et al.* [1987] can be envisaged, but with the simple x-connectors replaced by commercially available Mach-Zehnder connectors. In these connectors there is the possibility, by application of voltage, to switch the relative phase between the beams and thus transfer all the energy to either one of the two ports. In view of the signal-to-noise calculation above, it seems that the gain by switching is only marginal, and one might as well use the pair-wise interferometer.

### 6. Pupil plane vs. image plane.

There is a significant difference between the number of pixels required if one directly images the object (by using an exit pupil which is a scaled version of the entrance pupil) or utilises pupil plane beam combination (by deducing the visibility on each base-line). Suppose we have some field-of-view  $f$  and the size of a resolution element is  $r$ . The number of pixels across the detector will be  $q = 4f/r$ , where the coefficient of 4 comes from the requirement to have four pixels per resolution element. For an extended wave-length band the number of pixels will be  $q = 4f\lambda_{max}/r\lambda_{min}$ , and for a square array

$$q^2 = \left(4\frac{f\lambda_{max}}{r\lambda_{min}}\right)^2 = \left(4\frac{f}{r}\frac{\lambda_{max}}{\lambda_{min}}\right)^2 \text{ pixels.}$$

where  $f/r$  is calculated at the same wave-length. Assuming a field-of-view of 1.5 arcsec, a resolution of 3.4 milliarcsec (both at 500 nm), and 100 – 1000 nm for the wave-length range, we get  $3 \times 10^8$  pixels in the detector. We could, however, split the light (by means of dichroic mirrors) into narrow bands, and have separate detectors at each band. If we construct five equal-width channels, the five detectors will have a total of  $6 \times 10^6$  pixels in them. This is an appreciable reduction at the cost of optical complexity and lower signal-to-noise (but with some gain in spectral resolution).

Turning now to the pupil plane case, let us start with the case of a rectangular detector of width  $p$  and length  $l$ . We assume  $N$  combined beams and  $S = (N - 1)(3N/2 - 1)$  possible fringe frequencies (although only some  $(N - 1)N/2$  are used, see § 4). We require again four pixels per resolution element, so  $p = 4S = 2(N - 1)(3N - 2)$ . The cross-direction is for dispersed light. For  $N$  beams,  $l = N(N - 1)/2$  bands are needed. Thus we have,

$$p \times l = 2(N - 1)(3N - 2) \times N(N - 1)/2 = N(N - 1)^2(3N - 2) \text{ pixels}$$

whence we infer that the total number of pixels, for 25 telescopes, is  $1.1 \times 10^6$ .

If we use the pair-wise beam combination scheme (§ 5), the detector is even smaller. Suppose that some optical path difference creates  $w$  fringes at each junction. The number of pixels is  $q = 4wN$  on the side, and the total is

$$q^2 = (4wN)^2 \text{ pixels}$$

with no integration time limitations. For 5 fringes per pattern and 25 telescopes, our detector will contain  $2.5 \times 10^5$  pixels.

Now consider temporal modulation of the beams. If the beams are arranged adjacent to each other in the exit pupil,  $p = 4N$ , and  $l = p = 4N$ . This is because we do not have to separate all the spatial frequencies as before. The detector now contains

$$p \times l = 4N \times 4N = 16N^2 \text{ pixels,}$$

which have to be read at four times the highest modulation rate. So for 25 telescopes and lowest modulation frequency of 100 hz, we have to read 10000 pixels at the rate of 16 khz, a very plausible requirement.

An important argument in favor – or against – pupil-plane interferometry is the kind of object that will be observed and the wave-length of observation. In the visible and ultra-violet we are usually limited by shot noise (although some detectors have additive noise). When forming direct images the noise at every point is local and signal dependant. Thus small details on top of a large background will be difficult to discern, but will be readily detectable against a dark background. On the other hand, measurement in the pupil plane creates uncorrelated noise, which spreads

evenly when transformed into the final image. Any detail that is fainter than this average level will not be detectable, regardless of the general intensity distribution [Ribak *et al.* 1988].

## 7. Summary.

Two options that exist for multi-telescope interferometry on a single structure, direct imaging and pupil-plane beam combination, seem to have many optical parameters in common. Some of the shared parameters are: large detectors ( $10^6$  to  $10^8$  pixels), limited field-of-view, medium-to-high telescope magnification, and seven to eight reflections per path. The differences between the two schemes are in the maximum number of telescopes and their sizes (both larger for the imaging case) and in the spectral resolution (much higher in the pupil plane). If one uses pupil plane combination, detector sizes can be decreased significantly using pair-wise combination or temporal beam modulation. These can also be translated into reduced optical parameters and tolerances.

A simulation of the non-redundant beam-combination case showed an almost total loss of phase information below  $5 \times 10^7$  integrated photons. We intend to compare it with the performance of the other schemes. A higher signal-to-noise ratio is expected for the pair-wise beam combination. Yet another subject to be probed is the quality of images obtained in the two domains – image plane and pupil plane, with regards to such parameters as side-lobes and background noise.

## Acknowledgement.

The work described here was carried out by the Jet Propulsion Laboratory, California Institute of Technology, under contract with the National Aeronautics and Space Administration.

## References.

- J M Beckers, E K Hege, and P A Strittmatter (1983), "Optical interferometry with the MMT", SPIE 444, 85–88.
- P Connes, F Roddier, S Shaklan, and E Ribak (1987), "Fiber-linked telescope arrays on the ground and in space", *ESA workshop on Optical Interferometry in Space* (Granada, Spain). Editors N Longdon and V David 73–83.
- A H Greenaway (1985), "Estimation of log modulus and phase of the Fourier transform of a photon-limited process", *Opt. Comm.* 54, 75–80.
- J E Noordam, A H Greenaway, J D Bregman, and R S le Poole (1987), "OASIS: a mission concept", *ESA workshop on Optical Interferometry in Space* (Granada, Spain). Editors N Longdon and V David 51–60.
- E Ribak, F Roddier, C Roddier, and J B Breckinridge (1988), "Signal-to-noise limitations in white light holography", *Appl. Opt.* 27, 1183–1186.
- F Roddier (1987), "Signal-to-noise ratios and beam combination", *ESA-NOAO workshop in Interferometric Imaging in Astronomy* (Oracle, Arizona). Editor J Goad 135–138.
- W A Traub and W F Davis (1982), "Coherent optical system of modular imaging collectors (COSMIC) telescope array: astronomical goals and preliminary image reconstruction results", SPIE 332, 164–175.
- J F Walkup and J W Goodman, "Limitations of fringe-parameter estimation at low light levels", *J. Opt Soc. Am.* 63, 399–407 (1973).

DISCUSSION

**J. NOORDAM:** I do not understand how you can distinguish the fringes from a 25-telescope array with only 1200 pixels in your detector (in one dimension). In our OASIS design we are limited to 9 telescopes with 1000 pixels.

**E. RIBAK:** This is due to the fact that the ratio of the longest to shortest baseline in the combined beams is only 36.9. This is obtained through the demand that the shortest baseline is 25 units, whereas in your design it was 1. Since the longest baseline is similar, the ratio of the two is proportional to the number of telescopes.